

Forecasting Atmospheric Rivers during CalWater 2015

JASON M. CORDEIRA, F. MARTIN RALPH, ANDREW MARTIN, NATALIE GAGGINI,
J. RYAN SPACKMAN, PAUL J. NEIMAN, JONATHAN J. RUTZ, AND ROGER PIERCE

BACKGROUND. *What is an atmospheric river?*

Atmospheric rivers (ARs) are broadly defined as long and narrow corridors of strong water vapor transport that are characterized by enhanced vertically integrated water vapor (IWV) and enhanced IWV transport (IVT) (e.g., Ralph et al. 2004; Neiman et al. 2008). The IWV and IVT corridors associated with ARs are typically >2,000 km long and 500–1,000 km wide, and they often represent areas of instantaneous poleward and lateral moisture transport in the warm sector of midlatitude cyclones (e.g., Ralph et al. 2006; Dacre et al. 2015). These corridors often extend from the subtropics into the extratropics and contribute substantially to the occurrence of orographic precipitation events over the western United States (Ralph and Dettinger 2012). AR-related precipitation events constitute a large portion (~30%–50%) of annual precipitation and play a primary role in water resources management and water supply across the western United States (e.g., Dettinger et al. 2011). In fact, California’s annual precipitation varies far more than most of the country, and 85% of the variance in

annual precipitation in northern California results from annual variations in the top 5% wettest days per year, which are mostly attributed to water vapor flux along landfalling ARs (Dettinger and Cayan 2014). The purpose of this paper is to highlight different tools that were developed and used to analyze and forecast the location, intensity, duration, and potential landfall of regions of water vapor transport along ARs during an observing campaign over the northeast Pacific during January–March 2015 named CalWater 2015.

What is CalWater? CalWater is a multiyear program of field campaigns, numerical modeling efforts, and scientific analyses focused on phenomena that are key to the water supply and associated extremes (e.g., drought, flood) across the western United States (Ralph et al. 2016). The first field phase of CalWater—that is, “CalWater 1”—which occurred during 2009–11, 1) increased the number of observations of precipitation and aerosols, among other parameters, in the Sierra Nevada, Central Valley, and coastal region in California via the installation of the western region National Oceanic and Atmospheric Administration (NOAA) Hydrometeorological Testbed (HMT-West; Ralph et al. 2013a); and 2) sampled ARs in the coastal and near-coastal environment with the U.S. Department of Energy (DOE) G-1 aircraft. The second field phase of CalWater—that is, “CalWater 2”—is a multiyear effort that included field campaigns during February 2014 and January–March 2015, and includes anticipated field campaigns during 2016–18. CalWater 2 collectively focuses on observations of the structure and intensity of ARs in the coastal and offshore environment over the eastern North Pacific. The CalWater 2 field campaign during January–March 2015 (CalWater 2015) employed four research aircraft: the NOAA G-IV and P-3 aircraft, the DOE G-1 aircraft, and the National Aeronautics and Space Administration (NASA) ER-2 aircraft, as well as the

AFFILIATIONS: CORDEIRA—Department of Atmospheric Science and Chemistry, Plymouth State University, Plymouth, New Hampshire; RALPH AND MARTIN—Center for Western Weather and Water Extremes, Scripps Institution of Oceanography, University of California, San Diego, La Jolla, California; GAGGINI AND SPACKMAN—Science and Technology Corporation, Boulder, Colorado; NEIMAN—Physical Sciences Division, NOAA/Earth System Research Laboratory, Boulder, Colorado; RUTZ—NOAA/NWS/Western Region Headquarters, Salt Lake City, Utah; PIERCE—NOAA/NWS/San Diego Weather Forecast Office, San Diego, California

CORRESPONDING AUTHOR E-MAIL: Jason M. Cordeira, j_cordeira@plymouth.edu

DOI:10.1175/BAMS-D-15-00245.1

©2017 American Meteorological Society

TABLE 1. List of individuals who participated on the AR forecast team, their respective affiliation, and their role in CalWater 2015.

| Individual | Affiliation | Role |
|-----------------|--|--|
| Jason Cordeira | Plymouth State University | Forecast team lead and lead forecaster |
| Natalie Gaggini | Science and Technology Corporation | Lead forecaster |
| Jonathan Rutz | NOAA/NWS/Western Region headquarters | Lead forecaster and NWS coordinator |
| Roger Pierce | NOAA/NWS/San Diego Weather Forecast Office | NWS coordinator |
| William Rasch | NOAA/NWS/Sacramento Weather Forecast Office | NWS coordinator |
| Paul Neiman | NOAA/ESRL | Forecaster |
| Brian Kawzenuk | Plymouth State University | Forecaster |
| Klint Skelly | Plymouth State University | Forecaster |
| Vanessa Almanza | University of Hawai'i at Mānoa | Forecaster |
| Michael Mueller | Cooperative Institute for Research in Environmental Sciences (CIRES), University of Colorado Boulder | Forecaster |

NOAA Research Vessel (R/V) *Ron Brown*, which carried other DOE sensors. The National Science Foundation and DOE also sponsored an overlapping major aerosol and cloud measurement experiment at the coast called the Atmospheric Radiation Measurement (ARM) Cloud Aerosol Precipitation Experiment (ACAPEX) during January–March 2015. Additional information on the scientific objectives of the CalWater field campaigns can be found in Ralph et al. (2016). Additional information on ACAPEX can be found online (www.arm.gov/research/campaigns/amf2015apex), and additional information on the DOE ARM facilities used in ACAPEX is found in Schmid et al. (2014).

Motivation and objective. Planning efforts by the CalWater 2015 Forecasting Working Group (Ralph et al. 2016) identified the specific forecast needs for field operations and led to the formation of a forecast team that provided timely forecasts of the location, intensity, duration, and possible landfall of ARs in the offshore and near-coastal environments in support of field activities. The team consisted of three early-career scientists who acted as lead forecasters, and additional forecasters from several academic institutions, two

NOAA National Weather Service (NWS) Weather Forecast Offices, the NOAA/NWS Western Region Headquarters, NOAA's Earth System Research Laboratory (ESRL), and the Science and Technology Corporation (Table 1). A complementary team of forecasters also comprised the aerosol forecast team for ACAPEX. The AR forecasts were used for short-term (~1–3 days) flight and ship planning activities and long-term (~1–2 weeks) strategic planning for observing ARs with a single platform or multiple coincident platforms. The remainder of this paper highlights different tools that were developed to better forecast the location, intensity, duration, and possible landfall of ARs, and their implementation during CalWater 2015.

THE AR PORTAL. An “AR portal” was developed for various applications and was first tested significantly during CalWater 2015 in order to analyze and forecast the intensity, duration, and landfall of ARs during the experiment. The AR portal contains archived and real-time observations, gridded analyses, and gridded numerical weather prediction (NWP) forecasts of AR-related information over the northeast Pacific and western United States (<http://arportal.ucsd.edu>). The observations on the AR portal during

TABLE 2. List of archived and real-time gridded analyses and gridded forecasts from the GFS that were available on the AR portal during CalWater 2015.

| Model | Analysis type | Analysis and forecast fields | Frequency and location |
|----------------------------------|----------------------------|---|---|
| GFS | Map | IWV | Every 3 h from 0 to 72 h |
| | | Eulerian IWV tendency and budget | Every 6 h from 72 to 168 h |
| | | IVT | Every 12 h from 168 to 240 h |
| | | Time-integrated IVT | Over two domains: domain 1 spanned 16–66°N, 160–110°W; domain 2 spanned 25–50°N, 140–115°W ¹ |
| | | Sea level pressure | |
| | | Precipitation rate | |
| | | 900-hPa wind vector | |
| | | 900-hPa potential temperature | |
| | | 900-hPa equivalent potential temperature | |
| | | 900-hPa geopotential height | |
| | | 850-hPa wind vector | |
| | | 500-hPa geopotential height | |
| | | 500-hPa wind vector | |
| | | 500-hPa absolute vorticity | |
| 300-hPa wind vector and isotachs | | | |
| GFS | Map | Total precipitation | 5- and 7-day totals over domain 1 |
| GFS | Cross section, time series | Water vapor flux | Every 6 h from 0 to 60 h |
| | | Freezing level | Along 135°, 130°, 125°, and 120°W for 25°–50°N |
| | | IWV and IVT magnitude | |
| GFS | Time–height, time series | Water vapor flux | Every 3 h from 0 to 72 h |
| | | Relative humidity | Every 3 h from 0 to 168 h |
| | | Wind vector | Locations every 1° latitude × 1° longitude over a domain spanning 30°–50°N, 115°–135°W |
| | | Freezing level | |
| | | 3-h precipitation | |
| | | IWV and IVT magnitude | |
| GEFS | Thumbnail maps | IVT magnitude and direction | Every 24 h from 0 to 384 h |
| | | | Over domain 1 |
| GEFS | Probability maps | Fraction of ensemble with IVT magnitude $\geq 250 \text{ kg m}^{-1} \text{ s}^{-1}$ | Every 24 h from 0 to 384 h |
| | | | Over domain 1 |
| GEFS | Time–latitude maps | Fraction of ensemble with IVT magnitude ≥ 250 or $\geq 500 \text{ kg m}^{-1} \text{ s}^{-1}$ | Every 6 h from 0 to 384 h |
| | | | For locations along coast |
| GEFS | Time series | Ensemble-member IVT magnitude | Every 6 h from 0 to 384 h |
| | | | For locations along coast |

¹ The domain was adjusted westward later in the field campaign in order to accommodate temporary flight activities based out of Hawaii.

CalWater 2015 included 1) Geostationary Operational Environmental Satellite (GOES) imagery provided by NOAA; 2) Special Sensor Microwave Imager (SSM/I)-derived total precipitable water imagery provided by the Cooperative Institute for Meteorological Satellite Studies (CIMSS); 3) gridded analyses and point observations of precipitation provided by the California–Nevada River Forecast Center, the National Weather Service Advanced Hydrologic Prediction Service, and the Community Collaborative Rain, Hail and Snow Network; and 4) multi-instrument observations from the Coastal Atmospheric River Monitoring and Early Warning System at Bodega Bay, Chico, and Colfax in California provided by the NOAA ESRL. The gridded analyses and forecasts on the AR portal during CalWater 2015 were created from NCEP Global Forecast System (GFS) and Global Ensemble Forecast System (GEFS) data provided by the NOAA National Operational Model Archive and Distribution System (NOMADS). All data manipulations and images were generated using the National Center for Atmospheric Research (NCAR) Command Language (NCAR 2016) and were hosted at the Center for Western Weather and Water Extremes at the Scripps Institution of Oceanography and at Plymouth State University. These gridded analyses and NWP forecasts complemented existing tools that were used by forecasters to identify analyzed and forecasted locations of ARs based on IWV provided by the Atmospheric River Detection Tool (ARDT; Wick et al. 2013) developed by the NOAA ESRL's Physical Science Division. A list of the AR-related GFS and GEFS gridded products that were created and that supported CalWater 2015 is provided in Table 2.

The AR-related gridded forecast products focus on identifying and tracking ARs over the northeast Pacific with attention to their structure, intensity, and orientation at landfall along the U.S. West Coast. The gridded forecast products feature plan-view, cross-sectional, and time series analyses and forecasts of the IWV; horizontal water vapor flux; and the IVT vector, among other parameters. A large number of the gridded analysis and forecast products illustrate the IVT vector, which has been used to study ARs since 2008 (Neiman et al. 2008). Note that a majority (75%) of IVT within ARs is confined to the lower 2.25 km of the troposphere, where heavy orographic precipitation may result in regions of water vapor flux that intersect mountainous terrain along the U.S. West Coast (Ralph et al. 2005). Cross-sectional analyses and forecasts were particularly helpful in

identifying the vertical distribution of water vapor flux relative to coastal terrain during periods with landfalling ARs. Further motivation for incorporating the IVT vector into the forecast process is provided by a pair of studies by Lavers et al. (2014, 2016) that demonstrate that the IVT distribution is potentially more predictable with ~1–2 days of advanced lead time over the North Atlantic and North Pacific Oceans than the corresponding NWP-derived quantitative precipitation forecast (QPF). These results suggest that NWP-derived forecasts of the IVT vector might provide enhanced situational awareness for ARs over the North Pacific and North Atlantic prior to landfall along the west coast of both Europe and the United States.

Common thresholds used for identifying ARs from gridded analysis and forecast data over the northeast Pacific include a combination of IWV values ≥ 20 mm and IVT magnitudes ≥ 250 kg m⁻¹ s⁻¹ as discussed in Rutz et al. (2014). The IVT distribution, however, is often used in order to better emphasize the transport of water vapor and its role in precipitation instead of just the presence of water vapor, illustrated by the IWV distribution. The daily average IVT magnitude (IWV) explains ~50% (~25%) of the variance in 24-h precipitation across the western United States (Rutz et al. 2014). The IVT magnitude ≥ 250 kg m⁻¹ s⁻¹ threshold is therefore chosen in part because ARs with IVT magnitudes ≥ 250 kg m⁻¹ s⁻¹ have a larger impact on precipitation distributions across the western United States than coinciding areas of IWV values ≥ 20 mm according to Rutz et al. (2014). These thresholds may not apply universally across all ocean basins, but they have shown viability in identifying the locations of ARs over the northeast Pacific and locations of landfalling ARs along the U.S. West Coast. Similar thresholds for water vapor flux have also been developed for observational data that cannot explicitly calculate IVT magnitude. For example, Neiman et al. (2009) and Ralph et al. (2013b) calculate the bulk upslope water vapor flux as the product of terrain-normal lower-tropospheric profiler-derived winds and IWV, and define AR conditions at coastal locations (i.e., landfall) in northern California as IWV ≥ 20 mm and bulk upslope water vapor flux ≥ 150 mm m s⁻¹. The bulk upslope water vapor flux explains up to 75% of the variance in total precipitation that results from forced saturated ascent during landfalling ARs at coastal locations in northern California (Ralph et al. 2013b).

Displays of IVT and other gridded forecast parameters were computed from the deterministic GFS and

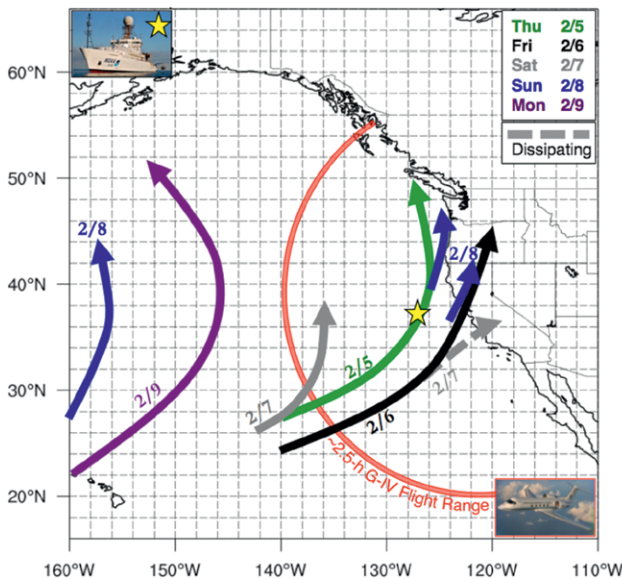
20-member GEFS data. The GEFS IVT forecasts were displayed as thumbnail and probability-over-threshold maps over the northeast Pacific, as multimember time series diagrams (e.g., a plume or dispersion diagram) for locations along the U.S. West Coast, and as a probability over threshold in a time–latitude framework for locations along the U.S. West Coast. The probability-over-threshold analysis is computed as the fraction of GEFS ensemble members with IVT magnitudes $\geq 250 \text{ kg m}^{-1} \text{ s}^{-1}$, and the time–latitude analysis follows latitude and longitude locations along the U.S. West Coast in lieu of locations along a meridian.

CALWATER 2015 IMPLEMENTATION.

Forecast process. The CalWater 2015 field campaign spanned from 12 January to 8 March 2015. The forecast team provided a weather briefing each morning from the field campaign operations center at McClellan Airfield outside Sacramento, California, to mission scientists at 0800 PST (i.e., 1600 UTC); each

weather briefing was preceded by a coordination call with the NWS at 0700 PST. The weather briefings focused on 1) the location and intensity of ARs that were platform targets over the northeast Pacific, and the timing and duration of AR conditions along the U.S. West Coast in both short-term (i.e., 1–3 days) and medium-term (i.e., 3–7 days) forecasts; 2) the probable locations and intensity of ARs over the northeast Pacific and along the U.S. West Coast in long-term forecasts (i.e., 7–10+ days); and 3) the local weather conditions for aircraft activities at the time of takeoff and landing. The weather briefings concluded with aerosol- and precipitation-related forecasts for the ACAPEX campaign and platform (flight, coastal observatories, and ship) planning activities. The weather briefings were followed by a detailed written summary of the weather briefing, and nowcasting support for flight activities that typically ended between 1600 and 2000 PST (i.e., between 0000 and 0400 UTC). These weather briefings and written summaries are also archived and available on the AR portal.

a. AR Continuity Forecast



b. Locations of HMT Network Observations

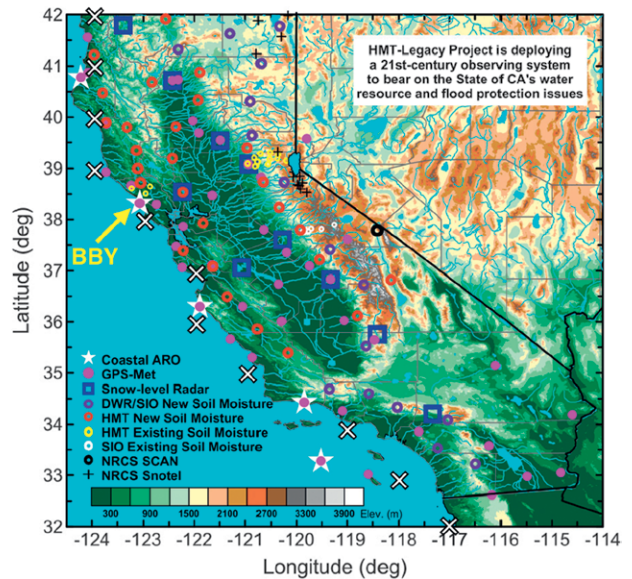


FIG. 1. (a) An example of the time continuity of AR corridors at 1600 PST (i.e., 0000 UTC; shown as bold lines, with the corresponding dates shown in m/d format, where m = month and d = day) used during CalWater 2015 for flight planning and field activities. The example was used in the forecast process on Thursday, 5 Feb 2015. The location of the NOAA R/V *Ron Brown* (yellow star) and the approximate 2.5-h flight range of the NOAA G-IV aircraft (red semicircle) are indicated. The sequence of green, black, and dashed gray arrows correspond to one propagating AR; the sequence of solid gray and smaller blue lines correspond to a second AR; and the longer solid blue and purple lines correspond to a third AR. (b) An annotated analysis of the HMT-West observing network as shown in Fig. 2b of White et al. (2013), with the location of the BBY ARO highlighted by the yellow arrow, and latitude and longitude locations that follow the U.S. West Coast in California used in Fig. 4 denoted by the “x” symbols.

Case study illustration of forecast and analysis tools. An example of a timeline and continuity graphic provided to mission scientists during the weather briefing on 5 February 2015 schematically illustrates the approximate location of AR corridors (i.e., forecaster-identified axes of $IVT \geq 250 \text{ kg m}^{-1} \text{ s}^{-1}$ from gridded forecast data) over the northeast Pacific during 5–8 February 2015 (Fig. 1a). The collocation of an AR corridor with the location of the NOAA R/V *Ron Brown* facilitated a coordinated multiplatform intensive operational period (IOP) over the northeast Pacific later

on 5 February 2015 that also included in situ observations by the NOAA G-IV and P-3, NASA ER-2, and DOE G-1 aircraft. This AR, and a subsequent AR, was further observed by campaign observing systems and the suite of instrumentation located across the HMT-West network (Fig. 1b) during landfall along the U.S. West Coast during 6–8 February 2015. A coastal atmospheric river observatory (ARO; White et al. 2009) site located at Bodega Bay (BBY) documented the landfall of these two ARs in association with two periods of enhanced $IWV \geq 20 \text{ mm}$ (values exceeded

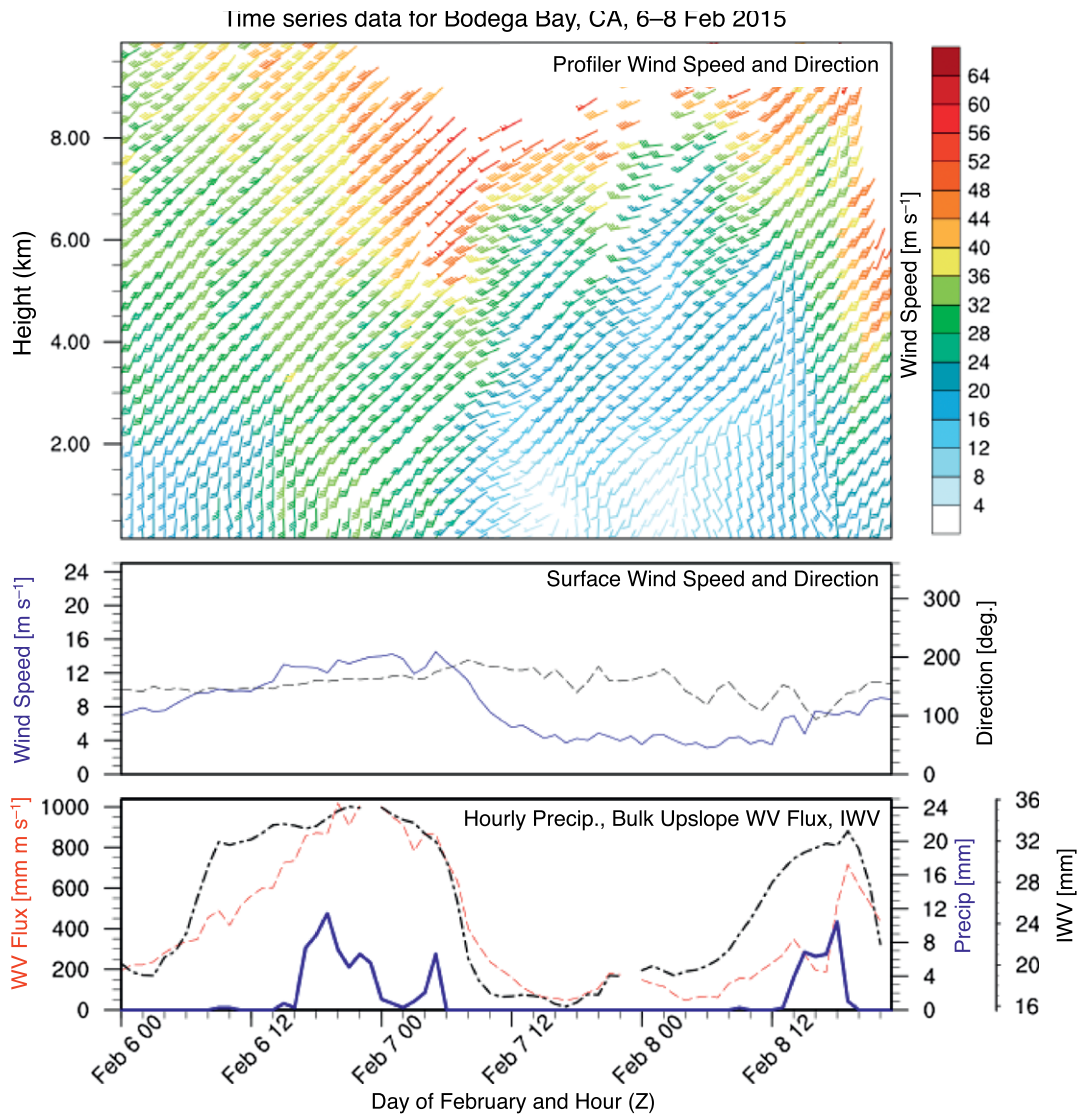


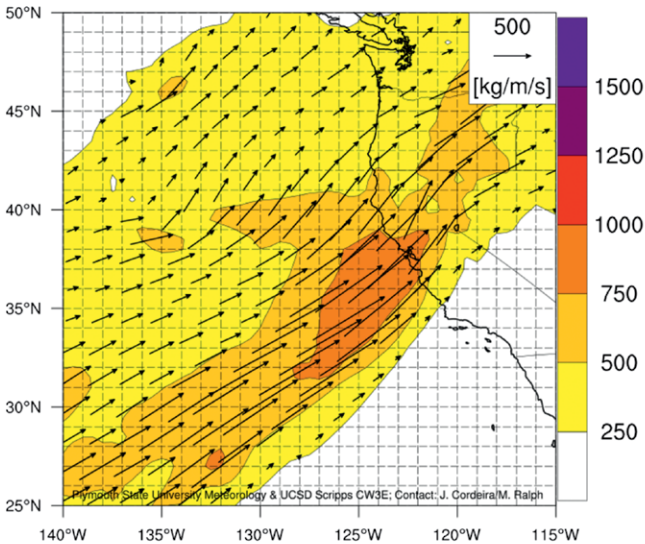
FIG. 2. Time series analysis of meteorological conditions at BBY for 6–8 Feb 2015. (top) Time–height analysis of horizontal wind from a 449-MHz profiler color shaded according to magnitude (m s^{-1}); (middle) surface wind speed (m s^{-1} ; blue line) and direction (dashed black line); and (bottom) bulk upslope water vapor flux (mm m s^{-1} ; red dashed line, calculated according to the methodology of Neiman et al. 2009), hourly precipitation (mm; blue line), and IWV (mm; black dashed contour).

30 mm), strong lower-tropospheric southwesterly flow, enhanced bulk upslope water vapor flux values $\geq 150 \text{ mm m s}^{-1}$ (values exceeded 800 mm m s^{-1}), and hourly precipitation amounts $> 8 \text{ mm h}^{-1}$ on 6–7 February 2015 and 8 February 2015 (Fig. 2).

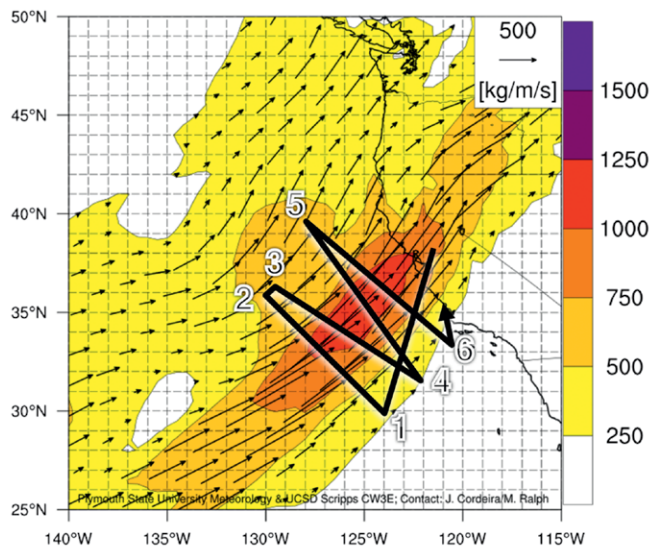
The shorter-term (~84 h) gridded GFS forecasts of the 6–7 February 2015 ARs were used for flight

planning purposes several days in advance. The deterministic 84-h gridded GFS forecast initialized at 1200 UTC 3 February 2015 illustrated the nose of a strong ($>750 \text{ kg m}^{-1} \text{ s}^{-1}$) corridor of southwest-to-northeast-oriented IVT along an AR over coastal regions of central California at 0000 UTC 7 February 2015 (Fig. 3a). The location and timing of this

a. 84-h IVT forecast valid 00Z 7 Feb 2015



b. 0-h IVT analysis valid 00Z 7 Feb 2015



c. GPS IWV, 0015 UTC 7 Feb 2015

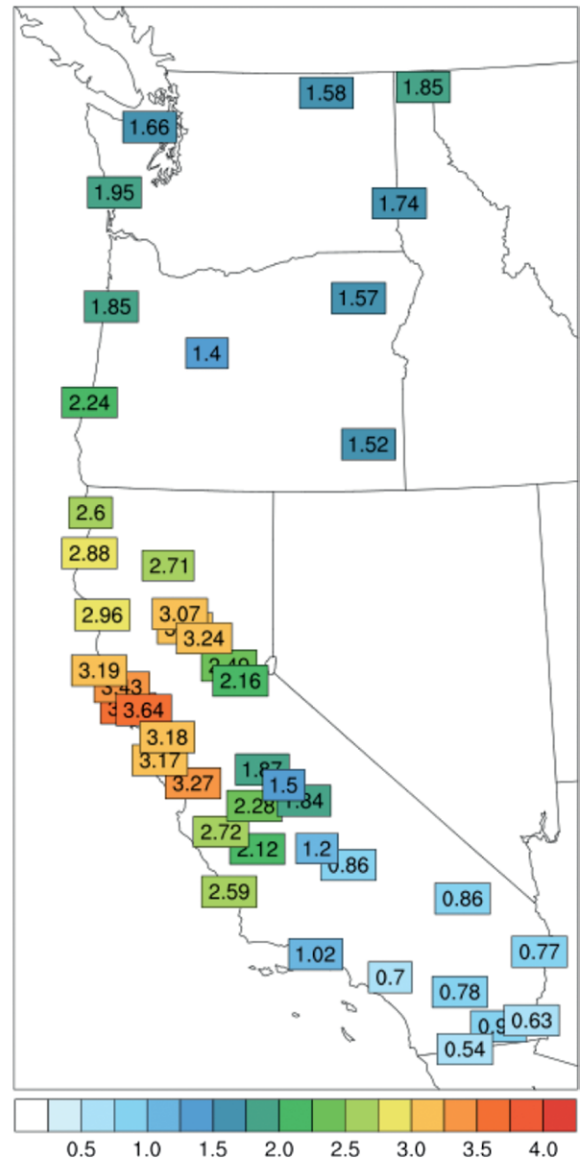


FIG. 3. (a) The 84-h NCEP GFS gridded forecast of IVT magnitude ($\text{kg m}^{-1} \text{ s}^{-1}$; shaded according to scale) and direction (vectors plotted according to scale and for magnitudes $\geq 250 \text{ kg m}^{-1} \text{ s}^{-1}$) initialized at 1200 UTC 3 Feb 2015. (b) As in (a), except for the verifying analysis of IVT magnitude and direction at 0000 UTC 7 Feb 2015 with overlaid draft flight track of the NOAA G-IV aircraft (the track follows the numbers in sequence as drawn where point 4 would correspond most closely in time to the aircraft location at 0000 UTC). (c) GPS-derived IWV (cm; shaded according to scale) at 0015 UTC 7 Feb 2015.

AR in the 84-h forecast verified within a very small margin of error (<100 km and <3 h) with respect to the 0-h analysis at 0000 UTC 7 February 2015, whereas the intensity of IVT along the AR was under forecast by >250 $\text{kg m}^{-1} \text{s}^{-1}$ (Fig. 3b; note the planned NOAA G-IV flight track based on the forecasted IVT distribution). Figure 3c provides an accompanying analysis of global positioning system–derived IWV observations across the western United States that is

available on the AR Portal that is also able to assist in verifying IWV-based definitions of AR conditions (e.g., IWV values ≥ 20 mm). The position error of this particular AR at landfall in the 84-h forecast is well below the average root-mean-square position error of ~ 500 km for global NWP models identified by Wick et al. (2013). Many locations along the U.S. West Coast, as well as California’s Sierra Nevada and Washington’s Cascades, ultimately received >100 mm

168-h GEFS IVT ($\text{kg m}^{-1} \text{s}^{-1}$) forecast initialized at 0000 UTC 31 Jan 2015, valid 0000 UTC 7 Feb 2015

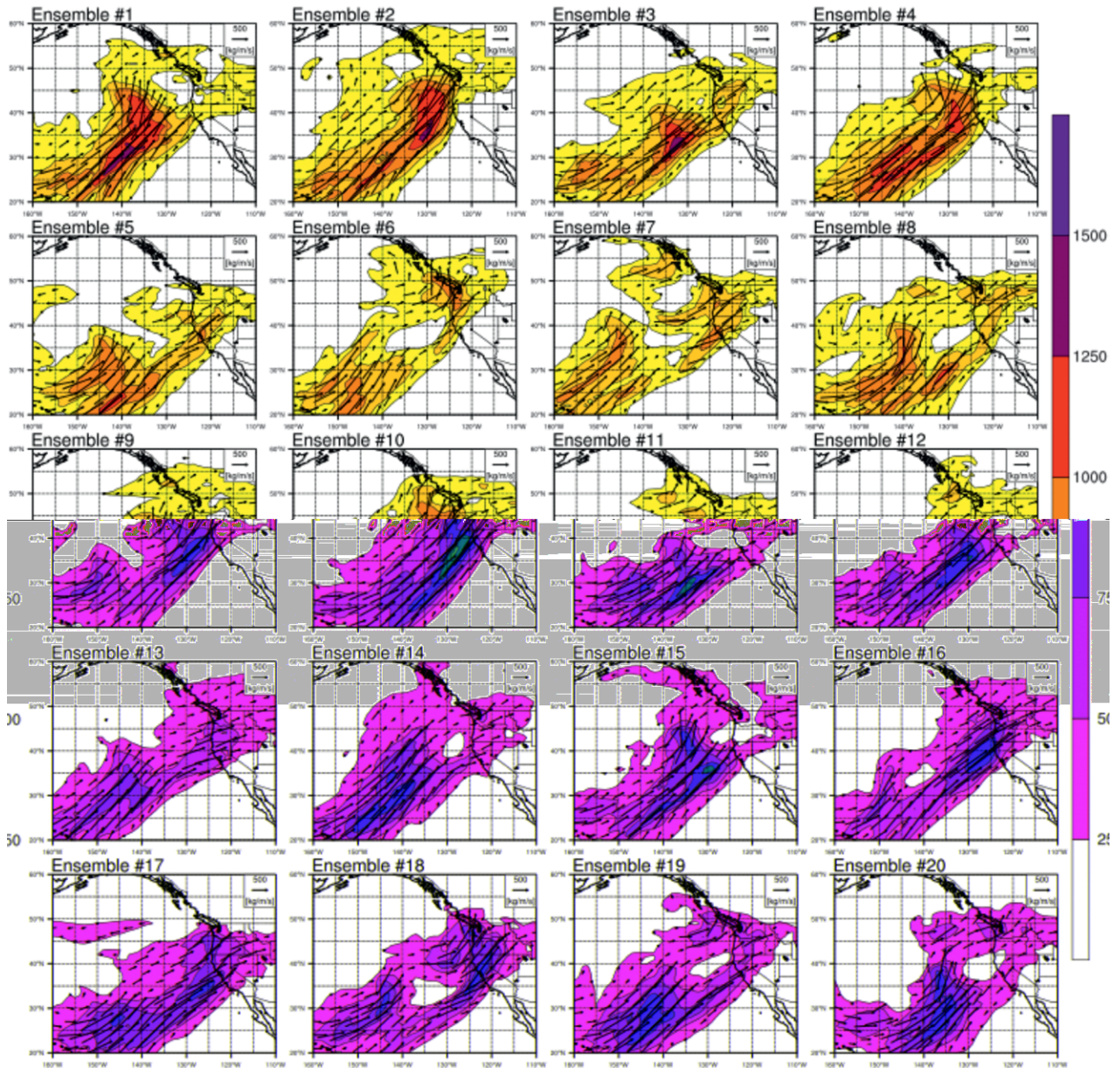


FIG. 4. The 168-h NCEP GEFS gridded forecasts of IVT (plotted as in Figs. 3a,b) initialized at 0000 UTC 31 Jan 2015 for each of the 20 ensemble members valid at 0000 UTC 7 Feb 2015.

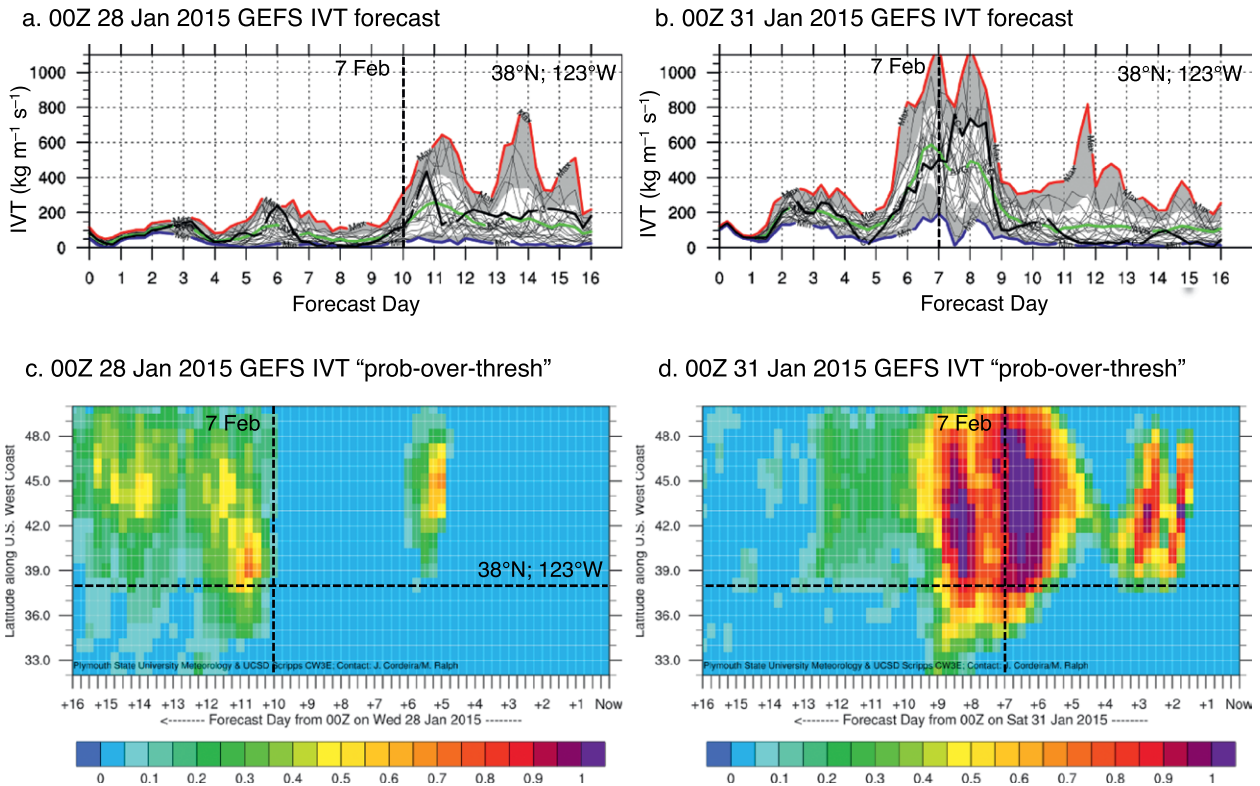


FIG. 5. Time series diagrams of the 16-day forecast of IVT magnitude ($\text{kg m}^{-1} \text{s}^{-1}$) at 38°N , 123°W initialized at (a) 0000 UTC 28 Jan 2015 and (b) 0000 UTC 31 Jan 2015 for each NCEP GEFS ensemble member (thin black lines), the control member (solid black line), and the ensemble mean (green line). The red and blue lines represent the maximum and minimum IVT magnitudes at each forecast hour, respectively; the white shaded regions represent the spread about the mean (plus/minus one standard deviation) of the ensemble at each forecast hour. A 16-day forecast time–latitude (where latitude follows the U.S. West Coast) depiction of the fraction of GEFS ensemble members (including the control member) with IVT magnitudes $\geq 250 \text{ kg m}^{-1} \text{ s}^{-1}$ is shown [shaded according to scale below panels (c) and (d)]. (a)–(d) The vertical dashed black lines denote the time of 0000 UTC 7 Feb 2015, whereas the dashed horizontal line denotes 38°N in (c) and (d). The latitude and longitude locations that follow the U.S. West Coast for California between 32° and 42°N are shown in Fig. 1b.

of precipitation during the 120-h period ending at 1200 UTC 9 February 2015; several locations received >400 mm of precipitation (not shown).

The longer-term gridded GEFS forecasts issued 1–2 weeks prior to the 5–8 February 2015 ARs were used to plan the coordinated multiplatform IOPs that took place offshore on 5 February 2015 and onshore during 6–8 February 2015 (Figs. 4 and 5). For example, the ensemble 168-h GEFS IVT thumbnail forecasts initialized at 0000 UTC 31 January 2015 illustrate overall agreement in the orientation (e.g., southwest to northeast) of IVT along an AR but considerable variability in the maximum intensity of IVT along an AR over the northeast Pacific (e.g., maximum IVT magnitudes range between 750 and

$>1,500 \text{ kg m}^{-1} \text{ s}^{-1}$) and in the timing of landfall (i.e., $\text{IVT} \geq 250 \text{ kg m}^{-1} \text{ s}^{-1}$ at coastal locations) at 0000 UTC 7 February 2015 (Fig. 4). Time series forecasts of 0–16-day ensemble-member IVT magnitude initialized at 0000 UTC 28 January 2015 (Fig. 5a) and at 0000 UTC 31 January 2015 (Fig. 5b) illustrate similar variability in the intensity and timing, and also duration of AR conditions ($\text{IVT} \geq 250 \text{ kg m}^{-1} \text{ s}^{-1}$) at 38°N , 123°W along the U.S. West Coast. The 0000 UTC 28 January 2015 GEFS forecast illustrated ensemble-member average IVT magnitudes $\geq 250 \text{ kg m}^{-1} \text{ s}^{-1}$ between \sim 0000 UTC 7 February 2015 and \sim 0000 UTC 8 February 2015 (\sim 24 h; Fig. 5a), whereas the 0000 UTC 31 January 2015 GEFS forecast illustrated ensemble-member average IVT magnitudes

$\geq 250 \text{ kg m}^{-1} \text{ s}^{-1}$ between ~0000 UTC 6 February 2015 and ~0000 UTC 9 February 2015 (~72 h; Fig. 5b). The GEFS thumbnail and time series forecasts suggested considerable uncertainty in the timing, duration, and intensity of AR conditions at coastal locations during 6–8 February 2015. This uncertainty is also illustrated via the corresponding 0–16-day GEFS time–latitude probability-over-threshold forecasts along the U.S. West Coast initialized at 0000 UTC 28 January 2015 (Fig. 5c) and 0000 UTC 31 January 2015 (Fig. 5d). This “AR landfall tool” highlighted probabilities of AR conditions ($\text{IVT} \geq 250 \text{ kg m}^{-1} \text{ s}^{-1}$) $> 50\%$ as early as ~10 days in advance for many locations along the U.S. West Coast, and when initializations were viewed in sequence every 6 h, provided valuable information on run-to-run consistency and increasing likelihoods of AR conditions beginning in north-coastal California and Oregon and proceeding south along the California coast over time.

SUMMARY. ARs are long and narrow corridors of enhanced IVT and IWV within the warm sector of extratropical cyclones that can produce heavy precipitation and flooding in regions of complex terrain, especially along the U.S. West Coast. ARs have been and continue to be the foci of several multiyear field campaigns under the CalWater umbrella (Ralph et al. 2016) that aim to better observe ARs over the eastern North Pacific, in the near-coastal and onshore environments. Forecasts of ARs for the CalWater 2015 field campaign made by a team of early-career scientists and participants from academic institutions and government agencies were informed by an AR portal that was created in order to provide a clearinghouse for observations, gridded analysis, and gridded forecast tools related to ARs over the northeast Pacific and over the western United States. The gridded analysis and forecast tools created for the CalWater 2015 field campaign provided valuable guidance for flight planning and other field activity purposes. These analyses and forecast tools, or adapted versions thereof, may also be useful in the day-to-day analysis and forecasts of ARs along the U.S. West Coast by weather forecasters and water managers to better anticipate hydrometeorological extremes. These adapted analyses and forecast tools may serve as a part of a decision support system that could provide AR-related forecasts for high-profile locations near reservoirs to aid in predicting water supply or forecast-informed reservoir operations (Ralph et al. 2014); vulnerable infrastructure as described by the 2009 Howard Hanson Dam flood risk

management crisis (White et al. 2012); watersheds to aid in streamflow prediction, floods, and flash floods (Neiman et al. 2011); or recent wildfire burn scars to aid in diagnosing debris flow or landslide susceptibility (White et al. 2013).

ACKNOWLEDGMENTS. The creation of the AR portal and participation for the lead author in CalWater 2015 was supported by NOAA Grant NA13OAR4830231 and the State of California Department of Water Resources Award 4600010378, both as part of broader projects led by the University of California, San Diego, Scripps Institution of Oceanography’s Center for Western Weather and Water Extremes. Student participation from Plymouth State University in CalWater 2015 was supported by NASA Space Grant NNX10AL97H. The authors are grateful for the comments provided by Benjamin Moore (University at Albany, State University of New York) and two anonymous reviewers, who greatly improved the quality of this manuscript.

FOR FURTHER READING

- Dacre, H. F., P. A. Clark, O. Martinez-Alvarado, M. A. Stringer, and D. A. Lavers, 2015: How do atmospheric rivers form? *Bull. Amer. Meteor. Soc.*, **96**, 1243–1255, doi:10.1175/BAMS-D-14-00031.1.
- Dettinger, M. D., and D. Cayan, 2014: Drought and the California Delta—A matter of extremes. *San Francisco Estuary Watershed Sci.*, 12(2). [Available online at <http://escholarship.org/uc/item/88f1j5ht>.]
- , F. M. Ralph, T. Das, P. J. Neiman, and D. Cayan, 2011: Atmospheric rivers, floods, and the water resources of California. *Water*, **3**, 445–478, doi:10.3390/w3020445.
- Lavers, D. A., F. Pappenberger, and E. Zsoter, 2014: Extending medium-range predictability of extreme hydrological events in Europe. *Nat. Commun.*, **5**, 5382, doi:10.1038/ncomms6382.
- , D. E. Waliser, F. M. Ralph, and M. D. Dettinger, 2016: Predictability of horizontal water vapor transport relative to precipitation: Enhancing situational awareness for forecasting western U.S. extreme precipitation and flooding. *Geophys. Res. Lett.*, **43**, 2275–2282, doi:10.1002/2016GL067765.
- NCAR, 2016: The NCAR Command Language Version 6.3.0. UCAR/NCAR/CISL/TDD, doi:10.5065/D6WD3XH5.
- Neiman, P. J., F. M. Ralph, G. A. Wick, J. D. Lundquist, and M. D. Dettinger, 2008: Meteorological

- characteristics and overland precipitation impacts of atmospheric rivers affecting the West Coast of North America based on eight years of SSM/I satellite observations. *J. Hydrometeorol.*, **9**, 22–47, doi:10.1175/2007JHM855.1.
- , A. B. White, F. M. Ralph, D. J. Gottas, and S. I. Gutman, 2009: A water vapour flux tool for precipitation forecasting. *Water Manage.*, **162**, 83–94, doi:10.1680/wama.2009.162.2.83.
- , L. J. Schick, F. M. Ralph, M. Hughes, and G. A. Wick, 2011: Flooding in western Washington: The connection to atmospheric rivers. *J. Hydrometeorol.*, **12**, 1337–1358, doi:10.1175/2011JHM1358.1.
- Ralph, F. M., and M. D. Dettinger, 2012: Historical and national perspectives on extreme West Coast precipitation associated with atmospheric rivers during December 2010. *Bull. Amer. Meteor. Soc.*, **93**, 783–790, doi:10.1175/BAMS-D-11-00188.1.
- , P. J. Neiman, and G. A. Wick, 2004: Satellite and CALJET aircraft observations of atmospheric rivers over the eastern North Pacific Ocean during the winter of 1997/98. *Mon. Wea. Rev.*, **132**, 1721–1745, doi:10.1175/1520-0493(2004)132<1721:SACAO>2.0.CO;2.
- , —, and R. Rotunno, 2005: Dropsonde observations in low-level jets over the northeastern Pacific Ocean from CALJET-1998 and PACJET-2001: Mean vertical-profile and atmospheric-river characteristics. *Mon. Wea. Rev.*, **133**, 889–910, doi:10.1175/MWR2896.1.
- , —, G. Wick, S. Gutman, M. Dettinger, D. Cayan, and A. B. White, 2006: Flooding on California's Russian River: Role of atmospheric rivers. *Geophys. Res. Lett.*, **33**, L13801, doi:10.1029/2006GL026689.
- , and Coauthors, 2013a: The emergence of weather-related test beds linking research and forecasting operations. *Bull. Amer. Meteor. Soc.*, **94**, 1187–1210, doi:10.1175/BAMS-D-12-00080.1.
- , T. Coleman, P. J. Neiman, R. Zamora, and M. D. Dettinger, 2013b: Observed impacts of duration and seasonality of atmospheric-river landfalls on soil moisture and runoff in coastal northern California. *J. Hydrometeorol.*, **14**, 443–459, doi:10.1175/JHM-D-12-076.1.
- , and Coauthors, 2014: A vision for future observations for Western U.S. extreme precipitation and flooding. *J. Contemp. Water Resour. Res. Educ.*, **153**, 16–32, doi:10.1111/j.1936-704X.2014.03176.x.
- , and Coauthors, 2016: CalWater field studies designed to quantify the roles of atmospheric rivers and aerosols in modulating U.S. West Coast precipitation in a changing climate. *Bull. Amer. Meteor. Soc.*, **97**, 1209–1228, doi:10.1175/BAMS-D-14-00043.1.
- Rutz, J. J., W. J. Steenburgh, and F. M. Ralph, 2014: Climatological characteristics of atmospheric rivers and their inland penetration over the western United States. *Mon. Wea. Rev.*, **142**, 905–921, doi:10.1175/MWR-D-13-00168.1.
- Schmid, B., and Coauthors, 2014: The DOE ARM aerial facility. *Bull. Amer. Meteor. Soc.*, **95**, 723–742, doi:10.1175/BAMS-D-13-00040.1.
- White, A. B., F. M. Ralph, P. J. Neiman, D. J. Gottas, and S. I. Gutman, 2009: The NOAA coastal atmospheric river observatory. Preprints, *34th Conf. on Radar Meteorology*, Williamsburg, VA, Amer. Meteor. Soc., 10B.4. [Available online at https://ams.confex.com/ams/34Radar/techprogram/paper_155601.htm.]
- , and Coauthors, 2012: NOAA's rapid response to the Howard A. Hanson Dam flood risk management crisis. *Bull. Amer. Meteor. Soc.*, **93**, 189–207, doi:10.1175/BAMS-D-11-00103.1.
- , and Coauthors, 2013: A twenty-first-century California observing network for monitoring extreme weather events. *J. Atmos. Oceanic Technol.*, **30**, 1585–1603, doi:10.1175/JTECH-D-12-00217.1.
- Wick, G. A., P. J. Neiman, F. M. Ralph, and T. M. Hamill, 2013: Evaluation of forecasts of the water vapor signature of atmospheric rivers in operational numerical weather prediction models. *Wea. Forecasting*, **28**, 1337–1352, doi:10.1175/WAF-D-13-00025.1.

AMS Education offers a new format option to view the AMS undergraduate course ebooks.

The WEBBOOK IS HERE!



Read with any web browser

Accessible anywhere with internet access

Accessible on public computers

Ideal for labs with computers

Contains dynamic web-based features

Allows student highlighting and notetaking

ametsoc.org/webBooks